



Strength and stiffness of cold-formed steel purlins with sleeved and overlapped bolted connections

A.H. Fávero Neto ¹, L.C.M. Vieira, Jr., ²M. Malite ³

Abstract

A series of nine cold-formed steel Z sections with sleeved and overlapped bolted connections were tested in bending. These types of cross-section and connections are largely used in continuous multi-span cold-formed steel purlin systems. This paper aims to analyze the strength and stiffness of semi-continuous purlins subjected to flexure. Results show that strength is often limited by a plastic mechanism failure that develops at the end of the overlap or sleeve caused by a combination of distortional and local buckling. Out-of-plane forces introduced by the beam undergoing distortional buckling to the connection reduce the web rigidity. The loss of web rigidity induces an early development of local buckling in the compressed flange, which leads to a bending strength lower than the one found in a continuous beam; this observation contrasts with the common practice of considering sleeved and overlapped purlins as continuous purlins. However, the rotational stiffness of the system is highly affected by the length of the connection and by the bearing deformations around the bolt hole. In addition to the experiments, this paper also presents a numerical and analytical study of the strength and stiffness of sleeved and overlapped bolted connections.

1. Introduction

Long runs of cold-formed steel purlins are widely used in framing systems. There are two common methods of connecting two adjacent purlins: (i) by overlapping and bolting two members, an overlapped connection, and (ii) by bolting a short cold-formed steel member similar to the purlin that holds and connects both purlins, a sleeved connection. The continuity is advantageous since it redistributes the maximum moments from the mid-span to the supports and also reduces displacements.

¹ Masters Student, University of Sao Paulo, EESC and Researcher at the Institute for Technological Research (IPT), Brazil <alomir@ipt.br>

² Assistant Professor, University of New Haven, CT, USA <luizvieirajr@gmail.com>

³ Associate Professor, University of Sao Paulo, EESC, Brazil <mamalite@sc.usp.br>

In a traditional design method the connection is assumed to guarantee full continuity. The strength and stability check of the connection zone are determined by superposing the component sections (double purlin or sleeve and purlin).

Several research groups have investigated the continuity assumption and a succinct literature review is outlined in the following section. The literature review is subdivided according to the connection type.

1.1 Sleeved Connection

Moore (1990) documented a series of purlin tests on commonly used sleeved connections. The tests were carried out by the UK Building Research Establishment in response to the collapse of several cold-formed steel roofs during snowstorms in the winter of 1981-82. Moore (1990) shows that strength of the sleeved purlin is higher (12% to 58%) than a continuous purlins and the failure happens at the end of the connection. Moore (1990) also noted that for sleeved connections the relationship between moment and rotation is non-linear. This characteristic is attributed to slip between purlin and sleeve, local yielding at the bolt hole, and distortion of the flange. Gutierrez et al. (2011) analyzing different sleeved connections observed that strength and stiffness can be lower than the one of continuous purlins.

Bryan (1993) determined an analytical equation for the rotational stiffness of sleeved connections based on a series of bolted lap shear tests. Tan et al. (2002) adapted Bryan's equations for different bolt diameters. Together, equations from Bryan (1993) and Tan et al. (2002) are a simplification of the behavior described by Moore (1990) since both equations lead to a linear moment-rotation relationship. Wang et al. (2012) proposed a model that takes in account the non-linearity of the moment-rotation relationship based on the results of lap shear test of single bolted connection.

1.2 Overlapped Connection

Murray and Elhouar (1994) concluded from 24 experiments of purlins with overlapped connections that the three traditional design assumptions are valid: (i) full continuity, (ii) lap strength is equal to the sum of individual strength of each purlin, and (iii) fully restrained bending (longitudinal stresses are determined by conventional flexure theory and lateral-torsional buckling is disregarded). These conclusions are the base for the design method proposed in the AISI Design Guide D111 (AISI, 2009). Ghosn and Sinno (1996) observed that failure is caused predominantly by bending and concluded that shear interaction can be disregarded. Epstein et al. (1998) concluded that the traditional design assumption of restrained bending may overestimate the strength, and that the inertia of each section of the purlin (lapped and not lapped) shall be carefully analyzed.

Ho and Chung (2004, 2006a, and 2006b) and Chung and Ho (2005) investigated a series of 26 overlapped-connection tests and observed failure at the edge of the lapped length due to the interaction between bending and shear. They also proposed an equation to determine the

rotational stiffness; this equation is based on experimental data of single-bolted lap shear tests. Zhang and Tong (2008) major contribution is the study of overlapped connections with self-drilling screws at the flanges. The additional screws on the flange do not change the strength of the connection arrangement. Dubina and Ungureanu (2010) recommend that instead of evaluating the ultimate capacity of an overlapped connection by an interaction between bending and shear, it should be evaluated based on the interaction bending and web crippling.

In order to further explore this topic the authors defined a series of nine bending tests of cold-formed steel Z sections with sleeved and overlapped bolted connections. The experiments are discussed in the next section.

2. Cold-formed steel Z purlins experiments

2.1 Design

The typical moment diagram of a continuous purlin is depicted in Figure 1(a). The uniform load represents dead, live, snow, and wind load. While the moment diagram varies depending on the connection stiffness, the inflection point is positioned at about a quarter of the purlin span from the support. At the region between inflection points, the moment diagram (parabola) can be approximated by a linear diagram, Figure 1(b). This linear approximation leads to the typical test setup used to study connection arrangements. The test setup is known as inverted purlin connection test and consists of a simply supported beam with a concentrated load at midspan, Figure 1(c).

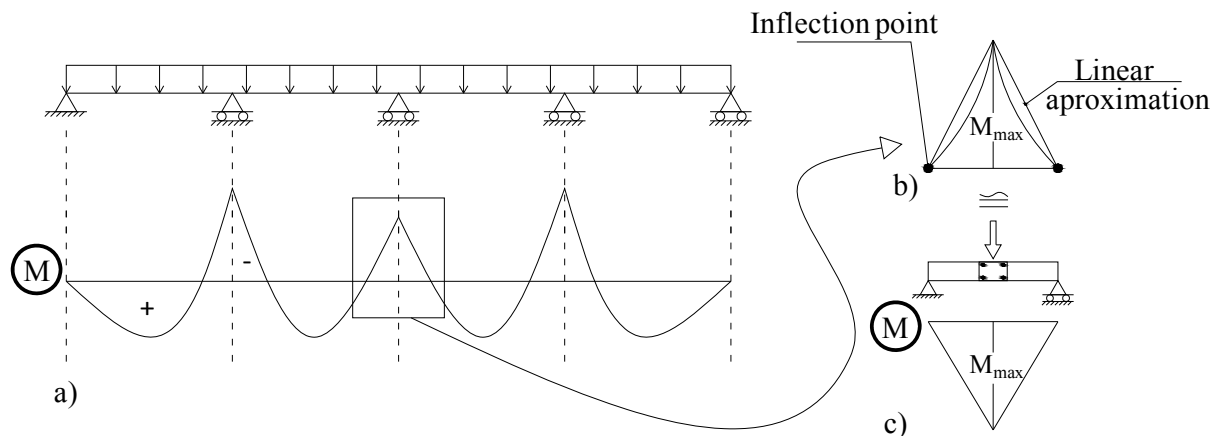


Figure 1 – Idealization of test setup. a) Moment diagram of a continuous purlin, b) Linear approximation of moment diagram, c) Test setup

Two different Z sections (Z1 and Z2) were tested; the sections have similar shape dimensions but different thickness. The nominal cross-section height is 270mm and the ratio between cross-section height and span length (length of 6,000mm) is 44, which lies in the typical range of 25 to 50. Each cross-section was tested with a sleeved connection and an overlapped connection; these

tests are also compared to a continuous specimen test. Information about cross-section dimensions, test set-up, and test results are summarized in Table 1.

The Z sections were tested in pairs and interconnected by the web to prevent the section from buckling laterally; the lateral bracing schedule is depicted in Figure 2(b). The load was applied under displacement control with a hydraulic actuator. More details on the loading apparatus and interconnection arrangement can be found in Fávero Neto and Malite (2012).

Table 1: Cross-section dimensions, connection information, peak load information, and failure mechanism

Cross-section	Specimen ¹	Cross-section Dimensions ²					Connection	Connection Length (mm)	Peak Load (kN)	Displacement at Peak Load (mm)	Limit State ³
		h (mm)	b ₁ (mm)	b ₂ (mm)	D (mm)	t (mm)					
Z1	Z1-C	269.5	81.57	72.60	19.72	1.71	None	-	20.6	35.6	D
	Z1-L5	269.5	82.83	73.29	18.44		Sleeve	1,036	17.7	38.1	D + L
	Z1-T5	269.2	82.29	72.68	19.32		Sleeve	1,036	19.6	40.6	D + L
	Z1-T11	270.0	81.5	72.23	19.74		Overlap	1,036	22.2	27.8	D + L
	Z1-L5P	268.2	81.85	72.41	19.48		Overlap	2,200	28.8	29.3	D
Z2	Z2-C	269.8	81.19	79.38	19.41	2.66	None	-	38.9	40.3	D
	Z2-L5	271.7	78.90	70.62	21.85		Sleeve	1,036	36.8	67.9	D of sleeve
	Z2-T5	271.2	79.04	70.21	21.81		Sleeve	1,036	48.0	42.7	D + L
	Z2-T11	271.8	79.04	70.08	21.18		Overlap	2,200	49.5	31.7	D

1 – The specimen nomenclature follows the abbreviations: Z for lipped zed section, 1 for nominal thickness of 1.75 mm and 2 for nominal thickness of 2.70 mm, C for continuous specimen, L for sleeved connection, and T for overlapped connection, 5 for connection length of 1,036mm, 11 for connection length of 2,200mm, and P for the second test of the same configuration

2 – Out-to-out average cross-section dimensions, where h is the height, b₁ is the compression flange width, b₂ is the tension flange width, D is the lip length, and t is the nominal thickness without the zinc coating.

3 – D stands for distortional buckling, D + L stands for distortional buckling followed by local buckling, D of sleeve stands for distortional buckling of the sleeve only.

2.2 Instrumentation

Five position transducers placed equidistant from each other measured the vertical displacement in the connection region and two other position transducers measured eventual support settlement or local deformation at the support region, Figure 2(a). At the center of the overlap, eight strain gages were placed, two on each exposed side of the flange (not in contact with the other section), while for sleeved connections only four strain gages were placed at the midspan, Figure 2(c). Four other strain gages were placed at the end of the connection, two on the top of upper flange and two on the bottom of the lower flange, Figure 2(d). Also a triaxial strain gage rosette was placed close to the corner of web and flange (compression zone) shown in Figure 2(d).

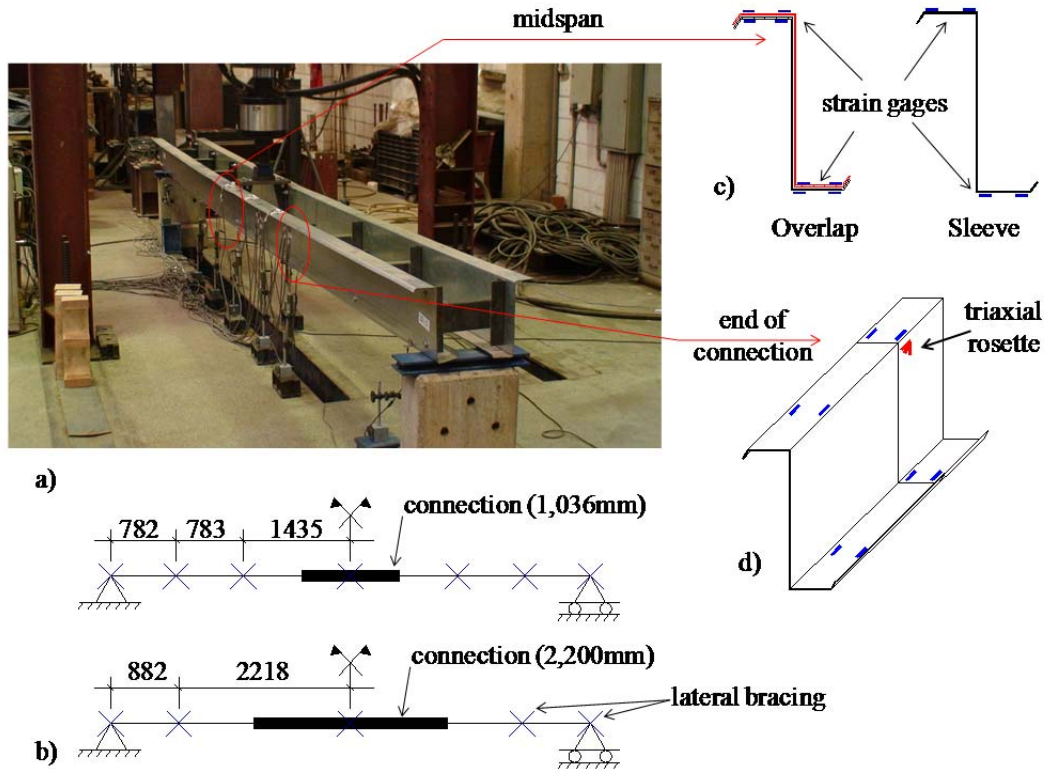


Figure 2 – Test instrumentation schematic and lateral bracing system schematics.

2.3 Steel Properties

All the specimens were fabricated with ZAR345 steel (ABNT, 2010). ZAR345 steel is coated with 0.02mm of zinc on each side of the steel plate. Three coupons of each steel thickness were sampled and tested according to ASTM E 8M (ASTM, 2011) to determine material characteristics. A summary of the yield stress (f_y) and ultimate stress (f_u) is given in Table 2.

Table 2: Coupon test results

Cross-section	Specimen number	Thickness	f_y (MPa)	f_u (MPa)
Z1	1	1.71	429.9	506.6
	2		438.2	515.5
	3		442.0	517.1
Z2	6	2.66	360.0	482.4
	7		337.5	476.9
	8		350.0	480.7

3. Results and discussion of experiments

The behavior and failure mode of these connections is consistent to those described in the literature. The interpretation, however, of the mechanism that leads to failure is different. At the connection region – sleeved or overlapped – two Z sections are stacked and connected on the

web by bolts as depicted in Figure 3(a). Figure 3(b) demonstrates how distortional buckling initially develops at the Z section stacked at the top of the arrangement. The section undergoing distortional buckling introduces out-of-plane forces and therefore lateral imperfection on the section stacked at the bottom of the arrangement. The web of the section at the bottom of the connection arrangement loses web rigidity and buckles locally at the compression zone, Figure 3(c). The additional imperfection applied on the compression zone reduces the member bending strength.

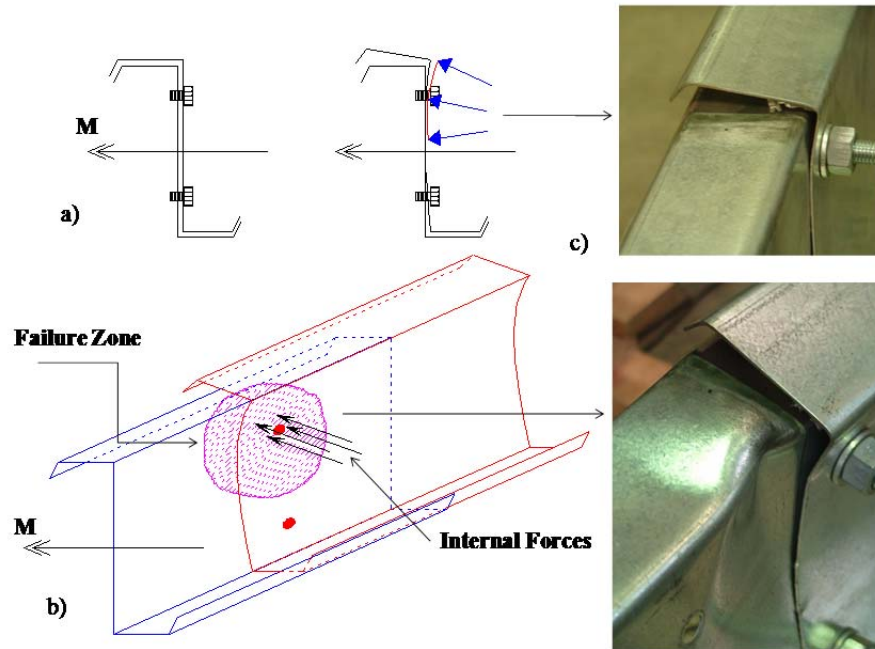


Figure 3 – Failure mechanism

Continuous purlins failed in distortional buckling, without developing a local failure at the corner of web and flange. In the experiment Z2-L5 only the sleeve buckled and no local buckling was observed. The overlap length showed to be an important factor on determining the failure mode, for longer overlap lengths the limit state was predominantly distortional buckling. Tests results of both connection arrangements are discussed separately in the next two sections.

3.1 Sleeved Connection

Sleeved connections presented lower strength and stiffness than continuous purlins and overlapped connections as summarized in Table 1. The sleeved connection arrangement resisted 14% less load than a continuous purlin for thinner section (Z1), and 5% less for the thicker sections (Z2). The failure mode in thinner sections (Z1) is the typical mechanism of distortional followed by local buckling. The same failure mode does not develop in specimens with greater thickness (Z2), which failed in distortional buckling of the sleeve only; due to the greater thickness, the lateral force exerted on the web when the sleeve is undergoing distortional buckling is not enough to trigger local buckling at the compression zone.

At peak load the vertical displacement of the sleeved connection is 10% higher than for continuous purlin in a thinner section (Z1), and 68% higher for thicker sections (Z2); so the designer shall carefully consider the vertical displacement in sleeved connections.

For thinner sections (Z1), an exploratory test was carried out (Z1-L5P). The lateral bracing system in Z1-L5P was connected close to the end of the connection, thus providing additional rigidity at the usual failure zone and consequently increasing the peak load by 10%. This observation is useful for detailing designers in that they should expect an increase of strength if lateral bracing or stiffener is placed close to the end of the connection.

3.2 Overlapped Connection

In addition to different thickness, for overlapped arrangements two different connection lengths were evaluated: (i) connection length of 1,036mm, identical to the sleeved connection, and (ii) longer connection arrangement of 2,200mm. The behavior and failure mode of the short connection length is the same mechanism described above – distortional followed by local buckling. For the longer connection length the specimens failed in distortional buckling. In thicker sections (Z2) there is only slight increase (3%) in the peak load for different connection lengths, but a considerable increase in the peak load (30%) when compared different connection lengths in thinner sections (Z1). This observation can be explained by the failure modes.

Distortional buckling develops in both connection lengths and introduces out-of-plane imperfections in the web. For short connection lengths an out-of-plane imperfection combined with longitudinal stresses leads to a premature local buckling failure. For long connection lengths, however, the failure zone (end of connection) is shifts to a region with lower longitudinal stresses and lower out-of-plane force/imperfection; this combination avoids local buckling at the compression zone.

4. Analytical Analysis

This section is concerned with the analytical prediction of strength and vertical displacement. While strength is evaluated using the Direct Strength Method (DSM) design approach, a new approach for predicting vertical displacement is proposed.

4.1 Displacement Prediction

Ho and Chung (2006) proposed that the total vertical displacement (Δ) can be subdivided in three components: (i) displacement due to bending moment (Δ_M), (ii) displacement due to shearing force (Δ_V), and (iii) displacement due to bearing deformation at the bolt hole (Δ_b). In addition to the components described by Ho and Chung (2006), if there is evidence of significant bolt slip, a component due to this effect (Δ_{slip}) shall also be considered. Thus the total vertical displacement is given by eq. (1).

$$\Delta = \Delta_M + \Delta_V + \Delta_b + \Delta_{slip} \quad (1)$$

In eq. (1) the components Δ_M and Δ_V can be determined for any connection arrangement via the virtual work method, eq. (2) and eq. (3).

$$1 \cdot \Delta_M = \int \frac{mM}{EI} dx \quad (2)$$

$$1 \cdot \Delta_V = \int K \left(\frac{vV}{GA} \right) dx \quad (3)$$

where:

1 = external virtual unit load in the direction of Δ_M or Δ_V ,

m, M = internal virtual moment, and internal moment, respectively,

E = modulus of elasticity of the material,

I = moment of inertia of cross-sectional area,

v, V = internal virtual shear, and internal shear, respectively,

K = form factor of the cross-sectional area,

G = shear modulus of elasticity,

A = cross-sectional area.

The bearing deformation component (Δ_b) and the bolt slip component (Δ_{slip}), however, require an understanding of the local deformations and the relative displacement developed in each connection arrangement. This topic is discussed separately in the next two sections.

4.1.1 Overlapped Connection

Ho and Chung (2006) present a complete discussion on displacement prediction of overlapped connections; the authors propose the approach described above to find Δ_M and Δ_V and they also present the moment and shear diagram to be used in eq. (2) and eq. (3) for overlapped connections. Furthermore, the center of rotation is assumed to occur at midspan (center of bolt group).

Since the bending moment at the center of rotation is the same as the bending moment at midspan, the force at each bolt hole (F_b) can be determined by eq. (4).

$$4. F_b \cdot r = M \rightarrow F_b = \frac{PL}{16r} \quad (4)$$

where:

M = bending moment at center of rotation, which for overlapped connection is equal to the bending moment at midspan ($PL/4$),

r = distance between bolt and center of bolt group,

P = concentrated load applied at midspan,

L = length of span.

The bearing deformation component (Δ_b) is proportional to the force at the bolt hole (F_b), given by eq. (5) in Ho and Chung (2006).

$$\Delta_b = \phi \cdot \frac{L}{2} = \frac{\delta_0}{r} \cdot \frac{L}{2} \quad (5)$$

where:

ϕ = joint rotation, which is the same as the ratio δ_0 / r ,

δ_0 = bearing deformation of each bolt hole under a bolt force (F_b),

From the equations derived in Ho and Chung (2006) the rotational stiffness of the overlapped connection, k_ϕ , is given by eq. (6).

$$k_\phi = \frac{M}{\phi} = \frac{PL}{4} \cdot \frac{r}{\delta_0} \quad (6)$$

Note that since the bearing stiffness (k_x) is given by the ratio between bolt force (F_b) and bearing deformation (δ_0), eq. (7), the bearing deformation (δ_0) can be expressed in terms of the bearing stiffness (k_x). Therefore the rotational stiffness (k_ϕ) is given by eq. (8):

$$k_x = \frac{F_b}{\delta_0} = \frac{PL}{16r} \cdot \frac{1}{\delta_0} \quad (7)$$

$$k_\phi = 4 k_x r^2 \quad (8)$$

Dubina and Ungureanu (2010) and Bryan (1993) consider a linear relationship between F_b and δ_0 . Chung and Ip (2001) and Wang et al. (2012), however, conclude that the relationship between F_b and δ_0 is nonlinear, but can be simplified to a multilinear relationship. Both models proposed in the literature lead to different predictions of δ_0 . The authors favored the Dubina and Ungureanu (2010) and Bryan (1993) models in their studies due to its simplicity, but recognize that more research should be conducted on this topic.

Bryan (1993) also mentions that bolt slip occurs and shall be taken in account when predicting joint displacement. Based on eq. (5) and assuming that instead of the bearing deformation (δ_0) there is bolt slip (δ_{slip}), eq. (9) gives the bolt slip displacement component (Δ_{slip}).

$$\Delta_{slip} = \frac{\delta_{slip}}{r} \cdot \frac{L}{2} \quad (9)$$

4.1.2 Sleeved Connection

The equilibrium of forces in the sleeved connection is significantly different than in the overlapped connection. In the sleeved connection there are two centers of rotation, Figure 4(a); one in the center of the bolt group of each purlin. The forces developed to transfer the moment from the purlin to the sleeve and back to the purlin are depicted in Figure 4(b). The idealized deformation mechanism developed at each bolt is depicted in Figure 4(c).

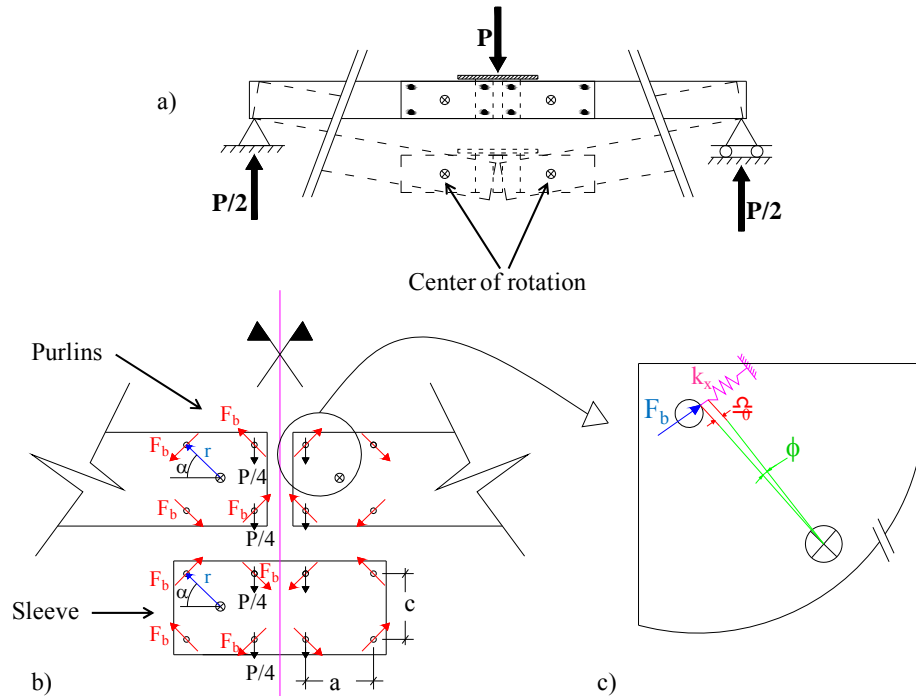


Figure 4 – Forces developed in the sleeved connection.

The equations developed for overlapped connection, with a few modifications, are also valid for sleeved connection analyses. The modifications include: (i) the displacement due to bending moment (Δ_M) and displacement due to shearing force (Δ_V) (eq. (2) and eq. (3)) shall consider the shear force diagram and bending moment diagram depicted in Appendix A, (ii) since in the sleeved connection the rotation center is not at the midspan, the bending moment (M) shall be replaced by the moment at the rotation center; for short sleeve, however, the moment at the rotation center can be assumed to be the same as the moment at midspan and thus the same equations derived for overlapped connection are valid.

The analytical solution provided above to determine the total vertical displacement (Δ) of overlapped and sleeved connection is involved, especially for the determination of the components Δ_M and Δ_V . The next section presents a simplified Finite Element (FE) beam model developed to determine the total vertical displacement (Δ).

4.1.3 Simplified model for displacement prediction of overlapped and sleeved connection

A FE beam model of the connection arrangement was generated using the MASTAN2 v3.3 software package (McGuire et al., 2000). The FE model consists of a single Z section beam and two nested Z sections at connection length – approximately twice the bending stiffness of a single section – and a rotational spring (k_ϕ) at the rotation center of the connection arrangement, Figure 5. The rotational spring (k_ϕ) of overlapped connection can be determined according to eq. (6) or eq. (8); for long-sleeved connections, the same equations shall be modified according to section 4.1.2.

The FE model automatically accounts for the displacement component due to bending moment (Δ_M). The displacement component due to bearing deformation at the bolt hole (Δ_b) is taken in account by means of the rotational spring. The FE model does not account for displacement due to shearing force (Δ_V) (usually negligible) and bolt slip deformation component (Δ_{slip}). These can be taken into account separately if deemed necessary.

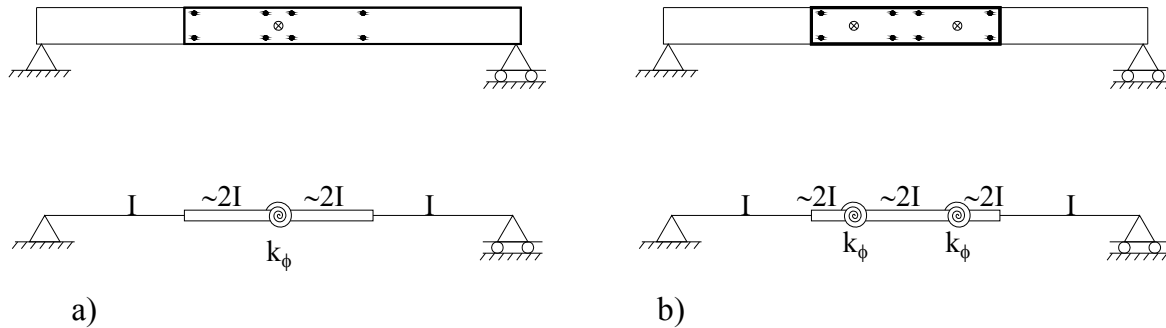


Figure 5 – Simplifications assumed in the numerical model. (a) Overlapped connection, (b) Sleeved connection

A condensed summary of the FE models is provided in Table 3. The displacement at the peak load in each test (Δ_{exp}) is compared to the displacement of the simplified FE beam model under the same load. Two FE simulations are compared: (i) first-order elastic analysis ($\Delta_{1st\ Order\ Elastic\ Analysis}$) and (ii) second order inelastic analysis that considers partial yielding accentuated by residual stresses ($\Delta_{2nd\ Order\ Inelastic\ Analysis}$). Model (i) resulted in an average displacement prediction 9% lower than the experimental results, while model (ii) lead to an average displacement prediction only 6% lower than the experimental results, thus suggesting that the simplified FE beam models, specially model (ii), reasonably predicts the total displacement of the connection arrangement. Note that the small difference can be attributed to the FE beam element not considering the loss of stiffness due to local or distortional buckling of the member.

Table 3: Displacement prediction using simplified model

Specimen	k_ϕ (kN.cm/rad)	Load (kN)	Δ_{exp} (cm)	$\Delta_{1st\ Order\ Elastic\ Analysis}$ (cm)	$\Delta_{2nd\ Order\ Inelastic\ Analysis}$ (cm)	Δ_{exp}	
						$\Delta_{1st\ Order\ Elastic\ Analysis}$	$\Delta_{2nd\ Order\ Elastic\ Analysis}$
Z1-C	-	10.30	3.56	2.78	2.82	1.28	1.26
Z1-L5	130,000	8.86	3.94	4.39	4.40	0.90	0.90
Z1-L5P	130,000	9.80	4.06	4.86	4.87	0.84	0.83
Z1-T5	565,000	11.10	2.78	2.75	2.77	1.01	1.00
Z1-T11	2,500,000	14.40	2.93	2.54	2.55	1.16	1.15
Z2-C	-	19.45	4.03	3.39	3.76	1.19	1.07
Z2-L5	223,000	18.28	6.80	5.53	5.63	1.23	1.21
Z2-T5	980,000	24.00	4.27	3.77	4.13	1.13	1.03
Z2-T11	4,300,000	24.75	3.17	2.80	2.89	1.13	1.10
Mean Value						1.10	1.06
CoV						0.14	0.13

4.2 Strength Prediction

The strength of continuous purlins is given by the interaction of shear forces and bending moment. The cross-section requires a check at midspan (double Z section) and at end of the connection arrangement (single Z section). For the connection arrangements studied in this paper the strength at the end of the connection is always critical and the midspan check can be disregarded.

In this paper, the nominal flexural strength (M_n) is determined according to the Direct Strength Method (DSM) prescribed in the AISI (2007). DSM relates the critical elastic buckling moments, local, distortional and global (M_{crL} , M_{crd} , M_{cre}), to the nominal flexural strength (M_n) of a beam. The nominal shear capacity (V_n) is also determined according to the AISI (2007). Table 4 summarizes the strength analysis of each specimen based on the measured dimensions and tests results. All specimens are considered fully braced i.e. lateral-torsional buckling will not occur and the nominal flexural strength for lateral-torsional buckling (M_{ne}) is equivalent to the yield moment (M_y). Elastic buckling analysis of the cross-section is performed using CUFSM (Schafer and Adany, 2006). For the thinner Z section (Z1) distortional buckling loads (M_{crd}/M_y) are slightly lower than local buckling loads (M_{crL}/M_y). For the thicker sections (Z2) local and distortional buckling loads are predominantly higher than the yield moment.

Table 4: Strength analysis for measured dimensions of each specimen

Specimen	M_y (kN.mm)	M_{crL}/M_y	M_{crd}/M_y	M_n (kN.mm)	M_{exp} (kN.mm)	V_n (kN)	V_{exp} (kN)	M_{exp}/M_n	V_{exp}/V_n
Z1-C	2703	0.52	0.47	1567	1546	17.2	5.2	0.99	0.30
Z1-L5	2703	0.52	0.44	1530	1099	17.2	4.4	0.72	0.26
Z1-L5P	2684	0.53	0.46	1553	1217	17.3	4.9	0.78	0.28
Z1-T5	2701	0.52	0.46	1554	1380	17.3	5.6	0.89	0.32
Z1-T11	2706	0.52	0.47	1569	1367	17.2	7.2	0.87	0.42
Z2-C	3371	1.55	0.95	2583	2920	65.7	9.7	1.13	0.15
Z2-L5	3315	1.57	1.09	2657	2285	65.3	9.2	0.86	0.14
Z2-T5	3302	1.58	1.09	2646	2976	65.4	12.0	1.12	0.18
Z2-T11	3298	1.57	1.07	2637	2352	65.2	12.4	0.89	0.19

The moment shear interaction diagram depicted in Figure 6 shows that except for the continuous purlins and test Z2-T5 the interaction curve leads to an unsafe strength prediction. Pham et al. (2012) reached similar conclusions for short lap length. The authors note that the difficulty in assessing the strength of a beam can be attributed to two factors: (i) the failure mechanism described in section 3 is not taken in account in the design and (ii) for non-continuous specimens, the longitudinal stress distribution considered in the buckling analysis is not the same as fully braced sections (simple flexure stress). In (i) the out-of-plane forces introduced on the web of the section considerably increase the imperfection on the compressed zone and thus decrease the member strength. By not taking in account factor (ii) the buckling analysis will not reflect the failure mode observed in the tests and thus leads to an incorrect strength prediction; this topic is discussed in more details in the next section.

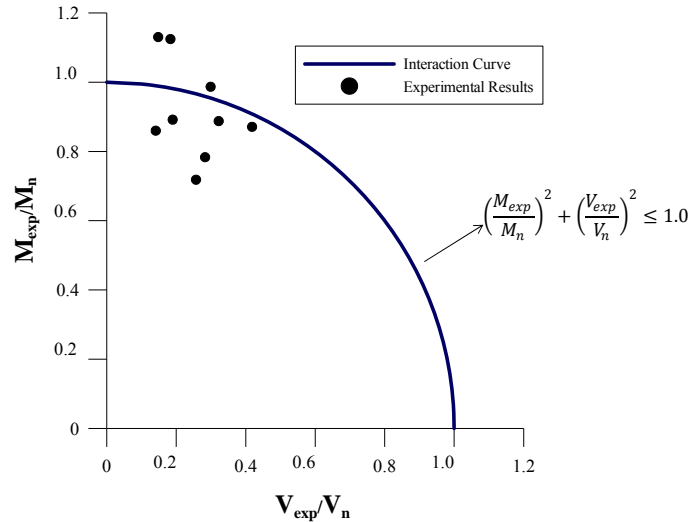


Figure 6 – Interaction diagram.

4.2.1 Numerical Analysis of longitudinal stresses

Traditional design practice suggests that, provided the section is fully braced, the longitudinal stress distribution is described by simple flexural stress ($\sigma=My/I$). The longitudinal stress distribution of a single section modeled by a shell element based finite element analysis in ANSYS (1997) is compared in Figure 7 to the theoretical values of symmetric and unsymmetric bending. For a single section with bracing only at the supports the stress distribution is similar to the theoretical stress distribution of unsymmetric bending. By adding two equally spaced lateral braces the longitudinal stress distribution changes from an unsymmetric to a symmetric bending stress distribution. Since in the experiments at least five lateral braces were provided, the structural designer is lead to conclude that simple flexural stress distribution correctly describes the longitudinal stress distribution. For the non-continuous members, however, the tests results revealed that the longitudinal stress distribution is not similar to simple flexural stress distribution.

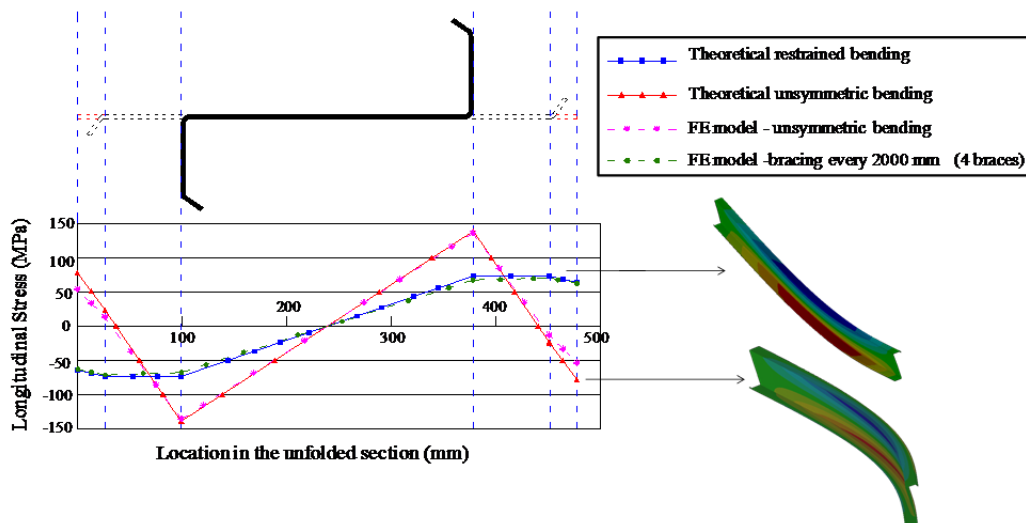


Figure 7 – Symmetric and unsymmetric bending analysis

In a simple flexural stress distribution case (restrained bending) the ratio of the stress at the strain gage placed close to the lip ($\sigma_{lip-flange}$) and the stress at the strain gage close to web ($\sigma_{flange-web}$) is equal to one. For unsymmetric bending the same ratio ($\sigma_{lip-flange}/\sigma_{flange-web}$) for any load level and the sections tested herein is close to 0.03. In Figure 8 the theoretical stress ratio ($\sigma_{lip-flange}/\sigma_{flange-web}$) is compared to the stress ratio measured at the midspan of tests Z1-C (continuous purlin) and Z1-L5 (sleeved connection). For the continuous purlin test the stress ratio in both flanges ($\sigma_{lip-flange}/\sigma_{flange-web}$) is similar to a simple flexural stress distribution, which reinforces the traditional design practice of considering a simple flexure stress distribution. Non-continuous assemblies, however, do not follow a simple flexure stress distribution and each flange has a different stress ratio $\sigma_{lip-flange}/\sigma_{flange-web}$. The compression flange in the test Z1-L5 presents a stress ratio very close to the stress ratio of unsymmetric bending, whereas the tension flange presents a stress ratio close to 0.3. In fact, the longitudinal stress distribution is highly influenced by the level of interaction between the two nested sections; this precludes the definition of a general stress ratio valid for any connection arrangement. Note that an incorrect longitudinal stress assumption will certainly compromise the strength prediction.

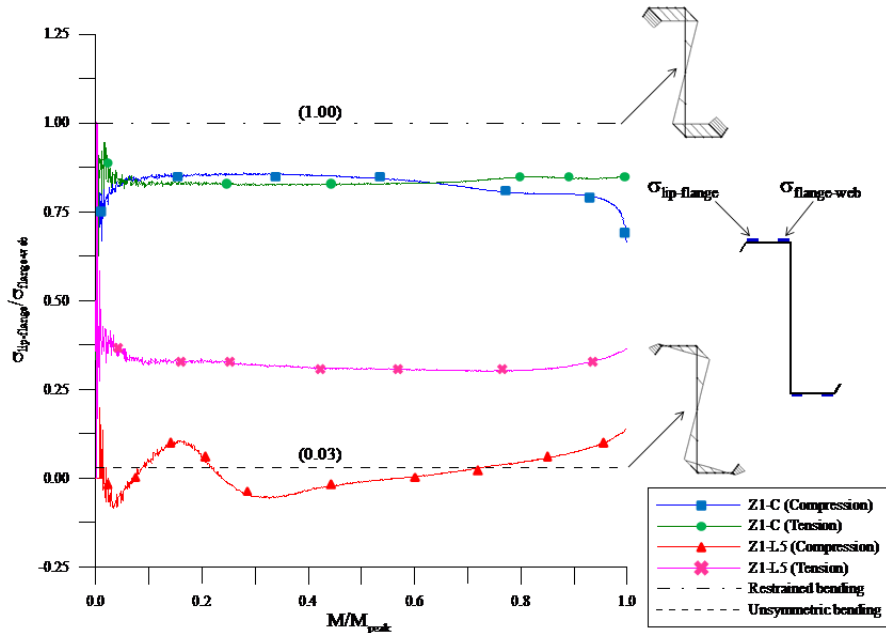


Figure 8 – Longitudinal Stress distribution in the experiments

5. Conclusions

Nine cold-formed steel Z sections with different connection arrangements were tested in bending. A short literature review of the topic was presented. The tests revealed a new understating of the failure mechanism of sleeved and overlapped connections; lateral forces introduced by the member undergoing distortional buckling amplify web imperfections of the neighbor cross-section and therefore reduces the strength of the arrangement. An analytical solution and a beam model for vertical displacement prediction were presented. The beam model leads to a simple and accurate method to predict vertical displacement. The design method prescribed in the AISI (2007) for combined bending and shear lead to an unsafe strength prediction. AISI (2007) does not take in account the interaction between the nested Z-section and

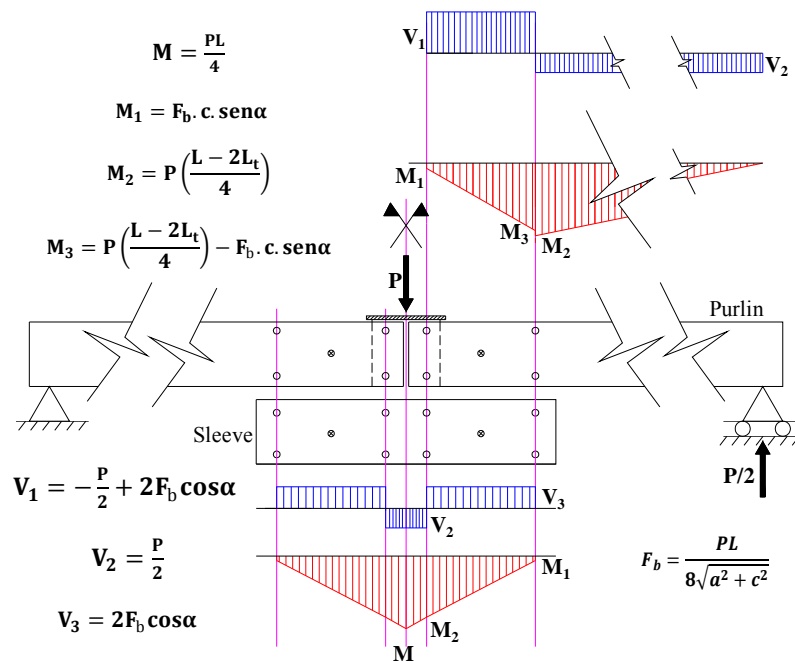
therefore the additional imperfection due to the lateral forces introduced in the system is disregarded. On the other hand, traditional design practice considers simple flexure stress distribution on the cross-section, whereas tests revealed that this assumption is only correct for continuous sections. For connections arrangements the interaction between the nested sections shall be taken in account to accurately represent the longitudinal stress distribution on the cross-section.

Acknowledgments

The authors are indebted to Coordination for the Improvement of Higher Education Personnel (CAPES) and National Council for Scientific and Technological Development (CNPq) for funding and Modular Building Systems for donating the specimens. The work reported herein was conducted by the first author as part of his master's thesis at Sao Carlos School of Engineering- University of Sao Paulo and while working at the Institute for Technological Research (IPT).

Appendix A

Shear force diagram and bending moment diagram for sleeved connection.



References

AMERICAN IRON AND STEEL INSTITUTE. (2007). **ANSI/AISI S100-2007**: North American Specification for the Design of Cold-Formed Steel Structural Members. Washington, DC.

_____. (2009). **D111-09**: Design Guide for Cold-Formed Steel Purlin Roof Framing Systems. Washington, DC.

AMERICAN SOCIETY FOR TESTING AND MATERIALS. (2011). **E8M**: Test methods for tension testing of metallic materials. West Conshohocken, PA.

ANSYS. User's guide for revision 5.5. Houston. v.1. 1997.

ASSOCIAÇÃO BRASILEIRA DE NORMAS TÉCNICAS (2010). **NBR 14762**: Design of cold formed steel structures. Rio de Janeiro. (In Portuguese).

BRYAN, E.R. (1993). The design of bolted joints in cold-formed steel sections. **Thin-Walled Structures**, v.16, p.239-262.

CHUNG, K.F.; HO H.C. (2005). Analyses and design of lapped connections between cold-formed steel Z sections. **Thin-Walled Structures**, v.43, p.1071-1090.

CHUNG, K.F.; IP, K.H. (2001). Finite element investigation on the structural behaviour of cold-formed steel bolted connections. **Engineering Structures**, v.23, p.1115-1125.

DUBINA, D.; UNGUREANU, V. (2010). Behaviour of multi-span cold-formed Z-purlins with bolted lapped connections. **Thin-Walled Structures**, v.48, p.866-871.

FÁVERO NETO, A. H.; MALITE, M. (2012). Analyses of the design procedure of steel purlins with continuity over the internal supports. Technical Report. Sao Carlos School of Engineering – USP. Sao Carlos. (In Portuguese).

GHOSN, A.A.; SINNO, R.R. (1996). Load capacity of nested, laterally braced, cold-formed steel Z-section beams. **Journal of Structural Engineering**, v.122, n.8, p.968-971.

GUTIERREZ, R.; LOUREIRO, A.; LOPEZ, M.; MORENO, A. (2011). Analysis of cold-formed purlins with slotted sleeve connections. **Thin-Walled Structures**, v.49, p.833-841.

HO H.C.; CHUNG, K.F. (2004). Experimental investigation into the structural behaviour of lapped connections between cold-formed steel Z sections. **Thin-Walled Structures**, v.42, p.1013-1033.

_____. (2006a). Analytical prediction on deformation characteristics of lapped connections between cold-formed steel Z sections. **Thin-Walled Structures**, v.44, p.115-130.

_____. (2006b). Structural behaviour of lapped cold-formed steel Z sections with generic bolted configurations. **Thin-Walled Structures**, v.44, p.466-480.

MOORE, D.B. (1990). Moment-rotation characteristics of purlin connections. In: **Proceedings of 10th International Specialty Conference on Cold-formed Steel Structures**. Saint Louis. University of Missouri-Rolla. p.525-544.

MCGUIRE, W.; Gallagher, R. H.; Ziemian, R. (2000). Matrix Structural Analysis, with MASTAN2. New York, Wiley.

MURRAY, T.M.; ELHOUAR, S. (1994). North American approach to the design of continuous Z- and C- purlins for gravity loading with experimental verification. **Engineering Structures**, v.16, n.5, p.337-341.

PHAM, C. H.; DAVIS, A. F.; EMMETT, B. R. (2012). Experimental and numerical investigations of high strength cold-formed lapped Z purlins under combined bending and shear. In: **Proceedings of 21st International Specialty Conference on Cold-Formed Steel Structures**. Saint Louis. Missouri University of Science and Technology. p.391-406.

SCHAFFER, B.W.; ADANY, S. (2006). Buckling analysis of cold-formed steel members using CUFSM: Conventional and constrained finite strip methods. In: **Proceedings of 18th International Specialty Conference on Cold-Formed Steel Structures**. Orlando, FL. p.39-54.

TAN, S.H.; SEAH, L.K.; LI, Y. (2002). Connections of sleeve joint purlin system. **Structural Engineering and Mechanics**, v.13, n.1, p.1-16.

WANG, C.J.; MYNORS, D.J.; MORGAN, T.; CARTWRIGHT, B. (2012). Deflection analysis of sleeve jointed purlin systems with non-linear rotational stiffness. **Applied Mechanics and Materials**, v.147, p.66-69.

ZHANG, L.; TONG, G. (2008). Moment resistance and flexural rigidity of lapped connections in multi-span cold-formed Z purlin systems. **Thin-Walled Structures**, v.46, p.551-560.